

# FGF19 Alleviates Cortisol-Induced Mitochondrial Damage and Apoptosis in Human Cardiomyocytes

Jingxian Zhang<sup>1</sup>, Xiaoping Meng<sup>1,\*</sup>

<sup>1</sup>Cardiology Department and Cardiac Rehabilitation Center, The Affiliated Hospital of Changchun University of Chinese Medicine, 130000 Changchun, Jilin, China

\*Correspondence: [Xvyaohui\\_yx@163.com](mailto:Xvyaohui_yx@163.com) (Xiaoping Meng)

Submitted: 18 June 2025 Revised: 19 August 2025 Accepted: 26 August 2025 Published: 20 October 2025

**Background:** Chronic stress-related disorders, such as cardiovascular neurosis, are frequently associated with elevated cortisol levels, which can impair mitochondrial function and contribute to cardiomyocyte injury. Fibroblast growth factor 19 (FGF19), a metabolic regulator with known cytoprotective properties, has been implicated in the maintenance of mitochondrial homeostasis. However, its role in mitigating cortisol-induced cardiac stress remains poorly understood. This study aimed to investigate whether FGF19 confers protection to cardiomyocytes against cortisol-induced mitochondrial dysfunction and apoptosis, and to elucidate the underlying molecular mechanisms.

**Methods:** Human AC16 cardiomyocytes were treated with cortisol and subjected to either FGF19 overexpression or knockdown. Cell viability, apoptosis, and mitochondrial function were evaluated using the 3-(4,5-dimethylthiazol-2-yl)-2,5-diphenyltetrazolium bromide (MTT) assay, terminal deoxynucleotidyl transferase dUTP nick-end labeling (TUNEL), adenosine triphosphate (ATP) quantification, mitochondrial DNA (mtDNA) copy number analysis, and mitochondrial membrane potential assessment using JC-1 dye, and reactive oxygen species (ROS) measurement. Western blot analysis was performed to examine the expression of proteins involved in mitochondrial biogenesis, including peroxisome proliferator-activated receptor gamma coactivator 1-alpha (PGC-1 $\alpha$ ) and mitochondrial transcription factor A (TFAM), as well as proteins regulating mitochondrial dynamics, such as Mitofusin 1 and 2 (Mfn1/2) and dynamin-related protein 1 (Drp1).

**Results:** Cortisol treatment significantly downregulated FGF19 expression, impaired mitochondrial function, and increased apoptosis ( $p < 0.01$ ). Overexpression of FGF19 enhanced mitochondrial biogenesis, preserved mitochondrial membrane potential, and reduced oxidative stress, thereby mitigating mitochondrial dysfunction and apoptosis ( $p < 0.01$ ). Conversely, FGF19 knockdown aggravated mitochondrial damage, elevated ROS levels, further reduced cell viability, and promoted apoptosis ( $p < 0.01$ ). The opposing phenotypes observed with FGF19 overexpression and silencing underscore its critical role in preserving mitochondrial integrity and promoting cell survival under cortisol-induced stress.

**Conclusion:** This study demonstrates that FGF19 mitigates cortisol-induced cardiomyocyte injury by improving mitochondrial function and reducing apoptosis. These findings provide experimental evidence supporting FGF19 as a potential therapeutic target for the treatment of cardiovascular neurosis and related stress-induced cardiac disorders.

**Keywords:** fibroblast growth factor 19; mitochondrial dysfunction; cortisol; cardiomyocyte apoptosis; cardiovascular neurosis

## Introduction

Cardiovascular neurosis, a common psychosomatic disorder, is characterized by cardiovascular symptoms such as palpitations, chest discomfort, and fatigue in the absence of identifiable organic pathology [1,2]. This condition has been increasingly associated with chronic psychological stress, which leads to elevated circulating cortisol levels. As a key component of the hypothalamic–pituitary–adrenal (HPA) axis response, elevated cortisol contributes to cardiomyocyte injury by promoting mitochondrial dysfunction and apoptosis [3,4]. However, despite its clinical significance, the molecular mechanisms underlying cortisol-induced mitochondrial impairment in cardiomyocytes remain incompletely understood.

Mitochondria are pivotal in energy metabolism, reactive oxygen species (ROS) regulation, and programmed cell death [5–7]. Disruption of mitochondrial homeostasis is central to various cardiovascular disorders, including ischemic heart disease, heart failure, and cardiomyopathy [8]. Mitochondrial dysfunction, characterized by reduced adenosine triphosphate (ATP) synthesis, depolarized membrane potential, increased ROS, and impaired mitochondrial biogenesis and dynamics, is a hallmark of stress-induced cardiac injury [9]. Critical regulators such as peroxisome proliferator-activated receptor gamma coactivator 1-alpha (PGC1 $\alpha$ ) and mitochondrial transcription factor A (TFAM) govern mitochondrial biogenesis, while mitofusins 1 and 2 (Mfn1/2) and dynamin-related protein 1 (Drp1) coordinate the fusion–fission processes essential for mitochondrial integrity [10,11].

Among the fibroblast growth factor family, both fibroblast growth factor 19 (FGF19) and FGF21 belong to the FGF19 subfamily but exhibit distinct biological functions and tissue specificities. FGF21 is primarily active in adipose tissue and the liver, and is well recognized for its potent antioxidative and anti-apoptotic effects in metabolic and cardiovascular diseases [12–14]. In contrast, FGF19 is mainly involved in the regulation of bile acid metabolism and glucose homeostasis; however, emerging evidence suggests that it may also confer cytoprotective effects under conditions of cellular stress [15–17]. Despite their structural similarities, FGF19 and FGF21 engage different signaling pathways and exert different tissue-specific effects. Preliminary studies have indicated that FGF19 can enhance mitochondrial function through activation of the AMPK/SIRT1 signaling pathway [18,19]. Nonetheless, its role in regulating cardiac mitochondrial function and promoting cardiomyocyte survival under glucocorticoid-induced stress remains largely unexplored.

The biological activity of FGF19 is primarily mediated through its canonical receptor fibroblast growth factor receptor 4 (FGFR4) and the co-receptor  $\beta$ -Klotho [12–14]. Notably, recent transcriptomic and proteomic analyses have confirmed the expression of FGFR4 in human cardiomyocytes, providing a mechanistic basis for FGF19 to exert direct effects on cardiac cells [20]. In this study, we employed the human AC16 cardiomyocyte cell line, which was established by the fusion of primary human ventricular cardiomyocytes with SV40-transformed fibroblasts [21]. AC16 cells retain key cardiac-specific markers and functional mitochondria, making them a widely accepted *in vitro* model for investigating cardiomyocyte biology and stress-related responses.

In this study, we investigate for the first time the role of FGF19 in protecting cardiomyocytes from cortisol-induced mitochondrial dysfunction and apoptosis. Utilizing both gain- and loss-of-function approaches, we aim to elucidate the mechanistic involvement of FGF19 in maintaining mitochondrial homeostasis and promoting cell survival under glucocorticoid stress. These findings may reveal novel molecular targets for therapeutic intervention in cardiovascular neurosis and other stress-related cardiomyopathies.

## Materials and Methods

### Cell Culture and Grouping

Human-derived AC16 cardiomyocyte cells used in this study were purchased from the cell repository of the Chinese Academy of Sciences (#SCSP-555). Cells were cultured in DMEM/F12 (#11330032, Gibco, USA) supplemented with 10% fetal bovine serum (FBS, #10099141C, Gibco, USA) and 1% penicillin-streptomycin (#15140122, Gibco, USA), and maintained at 37 °C in a humidified incubator with 5% CO<sub>2</sub>. Cell line authentication by short tandem repeat (STR) profiling and routine mycoplasma testing were performed to ensure cell identity and contamination-free status before experimentation.

To evaluate the functional role of FGF19 in cortisol-induced cardiomyocyte injury, AC16 human cardiomyocytes were seeded in 6-well plates at a density of  $2 \times 10^5$  cells per well and transfected at 70–80% confluence. Experimental groups were established as follows: (1) Control group: untreated cells; (2) CORT group: Cells treated with 10  $\mu$ M cortisol (#H0888, Sigma-Aldrich, USA) for 24 hours [22]; (3) CORT + vector group: Cells transfected with empty pcDNA3.1 vector (#20240516, constructed in-house, **Supplementary Table 1**) for 6 hours, followed by cortisol treatment for 24 hours; (4) CORT + FGF19 group: Cells transfected with a pcDNA3.1-FGF19 overexpression plasmid (#20250526, constructed in-house, **Supplementary Table 1**) using Lipofectamine 3000 (#L3000008, Thermo Fisher Scientific, USA) for 6 hours, followed by cortisol exposure for 24 hours; (5) CORT + si-NC group: Cells transfected with non-targeting siRNA (Sense: 5'-GCACCUCCAAUAAAGAUACACAUCA-3'; Antisense: 5'-UGAUGUGUAUCUUUAUUGGAGGUGC-3') for 6 hours, followed by cortisol treatment for 24 hours; (6) CORT + si-FGF19 group: Cells transfected with FGF19-specific siRNA (Sense: 5'-TCCATACGTGGACCACCACAC-3'; Antisense: 5'-GTGGTGGTGGTCACACGTATGGATC-3') under identical conditions, followed by cortisol treatment.

### qRT-PCR

Total RNA from AC16 cells in each experimental group was extracted using TRIzol reagent (#15596026, Invitrogen, USA) and reverse transcribed into cDNA using the PrimeScript RT reagent kit (#RR047A, Takara, Japan). Quantitative real-time PCR (qRT-PCR) was performed following the instructions provided with the SYBR Green PCR kit (#RR820A, Takara, Japan).

The amplification program consisted of an initial denaturation step at 95 °C for 30 s, followed by 40 cycles of 95 °C for 5 s and 60 °C for 30 s. The primer sequences for FGF19 were as follows: forward, 5'-TTGCCCTTCCCAAATCCCTC-3'; reverse, 5'-TTCTCAAGTTGTCCCAGGGC-3'.  $\beta$ -actin (forward: 5'-GGTCATCACTATTGGCAACGAGC-3'; reverse: 5'-CCAGACAGCACTGTGTTGGCATA-3') was used as the internal reference gene, and relative gene expression levels were calculated using the  $2^{-\Delta\Delta C_t}$  method. All experiments were performed in triplicate.

### Cell Viability Assay

Cell viability was assessed using the MTT assay. AC16 cells were first seeded into 96-well plates at a density of  $5 \times 10^3$  cells per well and cultured for 24 hours to allow cell attachment. Following experimental treatments in the same wells, 100  $\mu$ L of serum-free DMEM containing 5 mg/mL MTT (#M5655, Sigma-Aldrich, USA) was added to each well, and the cells were incubated at 37 °C in a 5% CO<sub>2</sub> humidified atmosphere for 4 hours. Following incubation, the culture medium was carefully removed,

and 150  $\mu$ L of dimethyl sulfoxide (DMSO; #D8418, Sigma-Aldrich, USA) was added to each well to dissolve the formazan crystals. The plates were gently agitated to ensure complete dissolution. Optical density (OD) was measured at 450 nm using a microplate reader (Thermo Fisher Scientific, USA). The OD values were used as a quantitative indicator of cell viability.

### TUNEL Assay

Apoptotic cells were detected using a TUNEL assay kit (#C1086, Beyotime, China) according to the manufacturer's instructions. Following experimental treatments, cells were fixed in 4% paraformaldehyde (#P0099, Beyotime, China) at room temperature for 30 minutes and then washed three times with PBS (5 minutes each). Permeabilization was performed using 0.3% Triton X-100 (#T8787, Sigma-Aldrich, USA) for 5 minutes at room temperature, followed by three additional PBS washes.

The TUNEL reaction mixture was prepared and applied to the cells, which were then incubated at 37 °C in the dark for 1 hour. Subsequently, nuclei were counterstained with 4',6-diamidino-2-phenylindole (DAPI; 1  $\mu$ g/mL; #C1002, Beyotime, China) for 5 minutes, and coverslips were mounted for imaging. TUNEL-positive cells were visualized using a fluorescence microscope (Olympus, Japan), and images were captured. For quantification, five random fields per group were selected, and the number of TUNEL-positive cells was counted to calculate the apoptosis rate.

### Biochemical Assay

Commercial assay kits were used to assess lactate dehydrogenase (LDH, #C0017, Beyotime, China) and creatine kinase-MB (CK-MB, #E006-1-1, Nanjing Jiancheng Bioengineering Institute, China) levels in the culture supernatant, as well as intracellular ATP levels (#S0026, Beyotime, China), mitochondrial DNA (mtDNA, #DP304, Tiangen Biotech, China), and mitochondrial membrane potential (JC-1, #C2006, Beyotime, China) in AC16 cardiomyocytes across different treatment groups.

Cell culture supernatants were first collected from each group for LDH and CK-MB analysis. According to the manufacturers' protocols, supernatants were incubated with the respective assay reagents at 37 °C for 30 minutes. Absorbance was then measured using a microplate reader at 450 nm for LDH and 340 nm for CK-MB. Standard curves were generated to calculate the concentrations of LDH and CK-MB.

For intracellular ATP quantification, cells were lysed using the lysis buffer provided in the ATP assay kit. The lysates were centrifuged, and the resulting supernatants were mixed with ATP detection reagents and incubated at 37 °C for 10 minutes. ATP levels were measured based on fluorescence intensity using a microplate reader.

Mitochondrial DNA content was determined by extracting total DNA and performing quantitative PCR

(qPCR) using specific primers for mitochondrial DNA (ND1 forward: 5'-TTAGCTCTCACCATCGCTC-3'; reverse: 5'-AGGTTAAAGGAGCCACTTATTAGTAAT-3') and nuclear DNA (GAPDH forward: 5'-GAAGGTGAAGGTCGGAGT-3'; reverse: 5'-GAAGATGGTGTATGGGATTTC-3'). The mtDNA/nDNA ratio was calculated to assess mitochondrial content.

Mitochondrial membrane potential was evaluated using the JC-1 fluorescent dye. Cells were incubated with JC-1 working solution at 37 °C in the dark for 20 minutes. Fluorescence was observed under a fluorescence microscope, with red and green emissions detected at excitation/emission wavelengths of 525/590 nm and 490/530 nm, respectively. The red-to-green fluorescence intensity ratio, indicative of mitochondrial membrane potential, was quantified using ImageJ software (version 1.53, NIH, Bethesda, MD, USA).

### Mitochondrial ROS Detection

Mitochondrial ROS levels were detected using MitoSOX™ Red (#M36008, Invitrogen, USA), a mitochondrial-targeted fluorogenic dye specific for superoxide. After treatment, AC16 cells were washed twice with warm Hank's Balanced Salt Solution (HBSS), then incubated with 5  $\mu$ M MitoSOX Red diluted in HBSS at 37 °C for 10 minutes in the dark. Following incubation, cells were washed three times with PBS to remove excess dye. Red fluorescence was observed using a fluorescence microscope (Olympus, Japan) with excitation/emission wavelengths of 510/580 nm. The mean fluorescence intensity of each group was quantified using ImageJ software (NIH, USA) and normalized to the control group. All experiments were performed in triplicate.

### Western Blot

Western blot was performed to detect the expression levels of relevant proteins. Total protein was extracted from cells using RIPA lysis buffer (#P0013C, Beyotime, China) supplemented with protease inhibitor (PMSF, #ST506, Beyotime, China) and phosphatase inhibitors to preserve protein integrity. Protein concentration was quantified using a BCA protein assay kit (#P0012, Beyotime, China). Equal amounts of protein (30  $\mu$ g) were separated by 10% SDS-PAGE and transferred onto PVDF membranes (#IPVH00010, Millipore, USA) at 100 V for 90 minutes using a wet transfer system (#1703930, Bio-Rad, USA).

Membranes were blocked in 5% non-fat milk at room temperature for 2 h, followed by overnight incubation at 4 °C with the following primary antibodies: FGF19 (1:1000, Abcam, ab225942), Bax (1:1000, Abcam, ab182733), Bcl-2 (1:1000, Abcam, ab182858), cleaved-caspase 3 (1:1000, Abcam, ab2302), PGC-1 $\alpha$  (1:1000, Abcam, ab191838), TFAM (1:1000, Abcam, ab176558), Drp1 (1:1000, Abcam, ab184247), Mfn1 (1:1000, Abcam, ab191853), Mfn2 (1:1000, Abcam, ab124773), and  $\beta$ -actin (1:1000, Abcam, ab8226) as the native control.

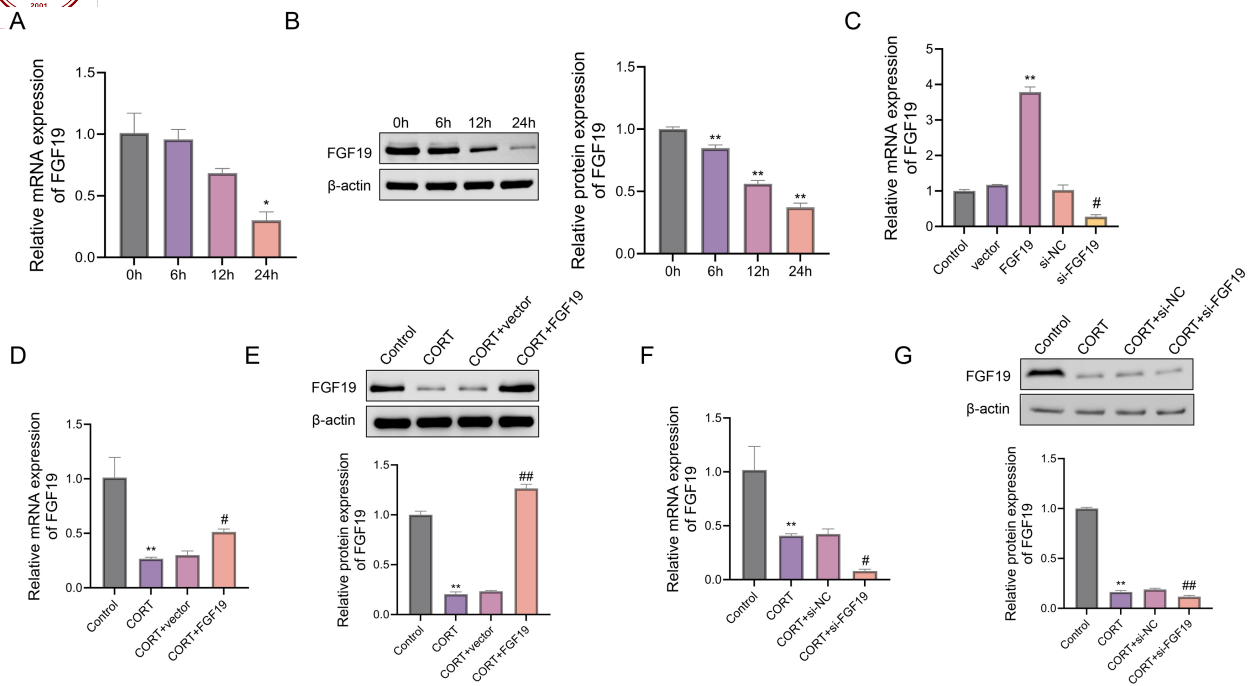


**Fig. 1. Cortisol suppresses FGF19 expression in AC16 cardiomyocytes.** (A,B) qRT-PCR (A) and Western blot (B) analyses showing time-dependent downregulation of FGF19 mRNA and protein levels in AC16 cells treated with 10  $\mu$ M cortisol for 0, 6, 12, or 24 hours. (C) qRT-PCR analysis of FGF19 mRNA levels in cells transfected with either FGF19 overexpression plasmid or FGF19-targeting siRNA (si-FGF19), compared to respective controls. (D,E) FGF19 mRNA (D) and protein (E) expression levels in cortisol-treated cells transfected with either vector or FGF19 overexpression plasmid. (F,G) FGF19 mRNA (F) and protein (G) expression levels in cortisol-treated cells transfected with si-NC or si-FGF19. Data are presented as mean  $\pm$  SD ( $n = 3$ ). \* $p < 0.05$ , \*\* $p < 0.01$  vs. 0 h, Vector, or Control; # $p < 0.05$ , ## $p < 0.01$  vs. si-NC, CORT + vector, or CORT + si-NC. FGF19, fibroblast growth factor 19; qRT-PCR, Quantitative real-time PCR; SD, standard deviation.

The next day, membranes were washed with TBST and incubated with HRP-conjugated secondary antibodies (1:5000, Abcam; goat anti-rabbit IgG-HRP: ab6721; goat anti-mouse IgG-HRP: ab6789) at room temperature for 1 hour. After washing, protein bands were visualized using enhanced chemiluminescence (ECL, #32106, Thermo Fisher, USA) and imaged with a Tanon 5200 Multi Imaging System (Tanon, China). Band intensities were quantified using ImageJ software (NIH, USA).

### Statistical Analysis

Statistical analyses were conducted using SPSS version 25.0 (IBM Corp., USA). The normality of data distribution was assessed using the Shapiro–Wilk test, and homogeneity of variances was evaluated using Levene’s test. Data that met the assumptions of normality and homogeneity were expressed as mean  $\pm$  standard deviation (SD). Comparisons among multiple groups were performed using one-way analysis of variance (ANOVA), followed by Tukey’s post hoc test. A  $p$ -value  $< 0.05$  was considered statistically significant. All experiments were conducted in at least three independent replicates unless otherwise specified.

## Results

### Cortisol Suppresses FGF19 Expression in AC16 Cells

To determine whether FGF19 expression is regulated under cortisol-induced stress, AC16 cardiomyocytes were treated with 10  $\mu$ M cortisol for varying durations. As shown in Fig. 1A, quantitative real-time PCR (qRT-PCR) revealed a significant time-dependent decrease in FGF19 mRNA expression. Compared to baseline (0 h), FGF19 transcript levels were markedly downregulated at 24 hours ( $p < 0.05$ ), while no significant changes were observed at 6 or 12 hours. Consistent with the transcriptional data, Western blot analysis confirmed a significant reduction in FGF19 protein levels from 6 to 24 hours post-cortisol exposure ( $p < 0.01$ ; Fig. 1B), supporting the presence of transcriptional repression.

To evaluate the efficiency of genetic modulation, FGF19 was either overexpressed via plasmid transfection or silenced using siRNA. As shown in Fig. 1C, FGF19 mRNA expression was significantly upregulated in the overexpression group and markedly suppressed in the si-FGF19 group, compared to their respective controls (vector and si-NC;  $p < 0.05$ ), confirming the effectiveness of the transfection protocols.

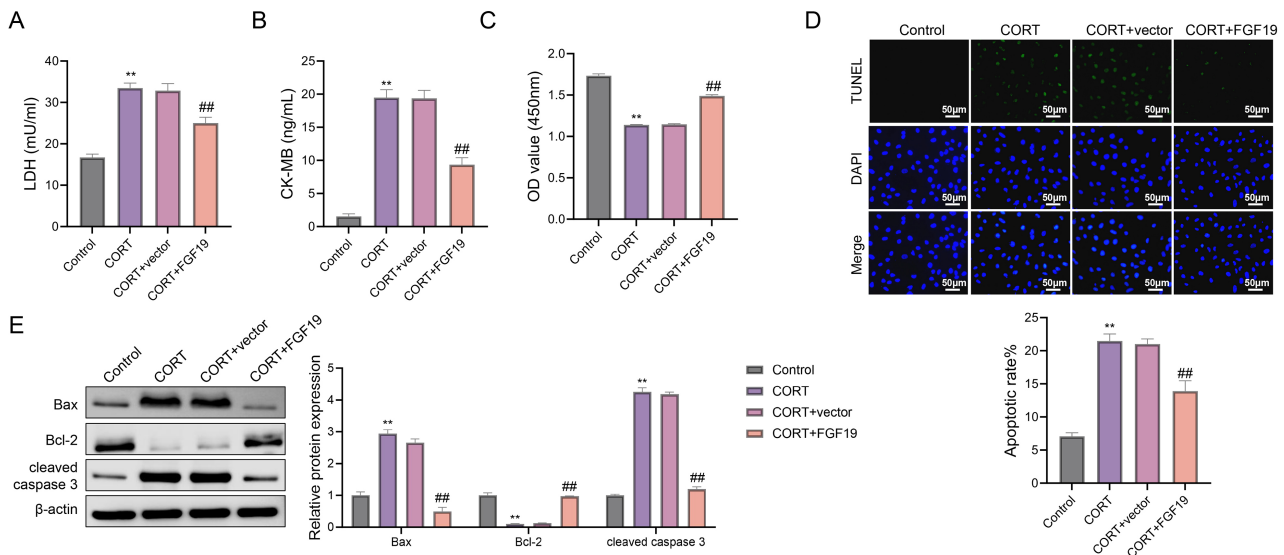


**Fig. 2. FGF19 overexpression attenuates cortisol-induced cellular injury and apoptosis in AC16 cells.** (A,B) Quantification of LDH (A) and CK-MB (B) levels in culture supernatants following treatment with cortisol and/or FGF19 overexpression. (C) Cell viability assessed by MTT assay. (D) Representative images of TUNEL/DAPI staining and quantification of apoptotic rate. Scale bar = 50  $\mu$ m. (E) Western blot analysis of apoptosis-related proteins, including Bax, Bcl-2, and cleaved caspase-3. Data are presented as mean  $\pm$  SD (n = 3). \*\* $p$  < 0.01 vs. Control; ## $p$  < 0.01 vs. CORT + vector. LDH, lactate dehydrogenase; CK-MB, creatine kinase-MB; MTT, 3-(4,5-dimethylthiazol-2-yl)-2,5-diphenyltetrazolium bromide; TUNEL, terminal deoxynucleotidyl transferase dUTP nick-end labeling; DAPI, 6-diamidino-2-phenylindole.

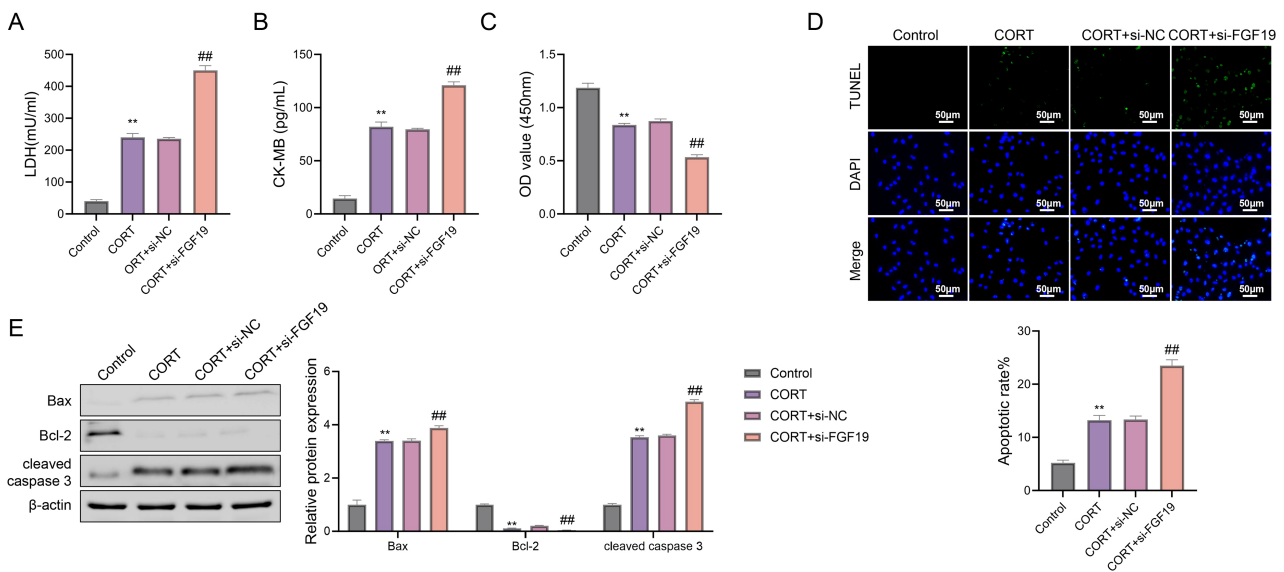


**Fig. 3. FGF19 knockdown exacerbates cortisol-induced cell injury and promotes apoptosis in AC16 cells.** (A,B) Quantification of LDH (A) and CK-MB (B) levels in the culture supernatants of cells transfected with siRNA targeting FGF19 under cortisol treatment. (C) Cell viability assessed by MTT assay. (D) Representative images of TUNEL/DAPI staining and quantification of apoptotic rate. Scale bar = 50  $\mu$ m. (E) Western blot analysis of apoptosis-related proteins, including Bax, Bcl-2, and cleaved caspase-3. Data are presented as mean  $\pm$  SD (n = 3). \*\* $p$  < 0.01 vs. Control; ## $p$  < 0.01 vs. CORT + vector.

Next, we assessed whether FGF19 expression could be effectively modulated under cortisol stimulation. As shown in Fig. 1D,E, FGF19 overexpression significantly increased both mRNA ( $p$  < 0.05) and protein levels ( $p$  < 0.01) in cortisol-treated cells compared to vector controls.

Conversely, Fig. 1F,G demonstrated that siRNA-mediated knockdown of FGF19 further reduced its mRNA ( $p$  < 0.05) and protein expression ( $p$  < 0.01) relative to the CORT + si-NC group.

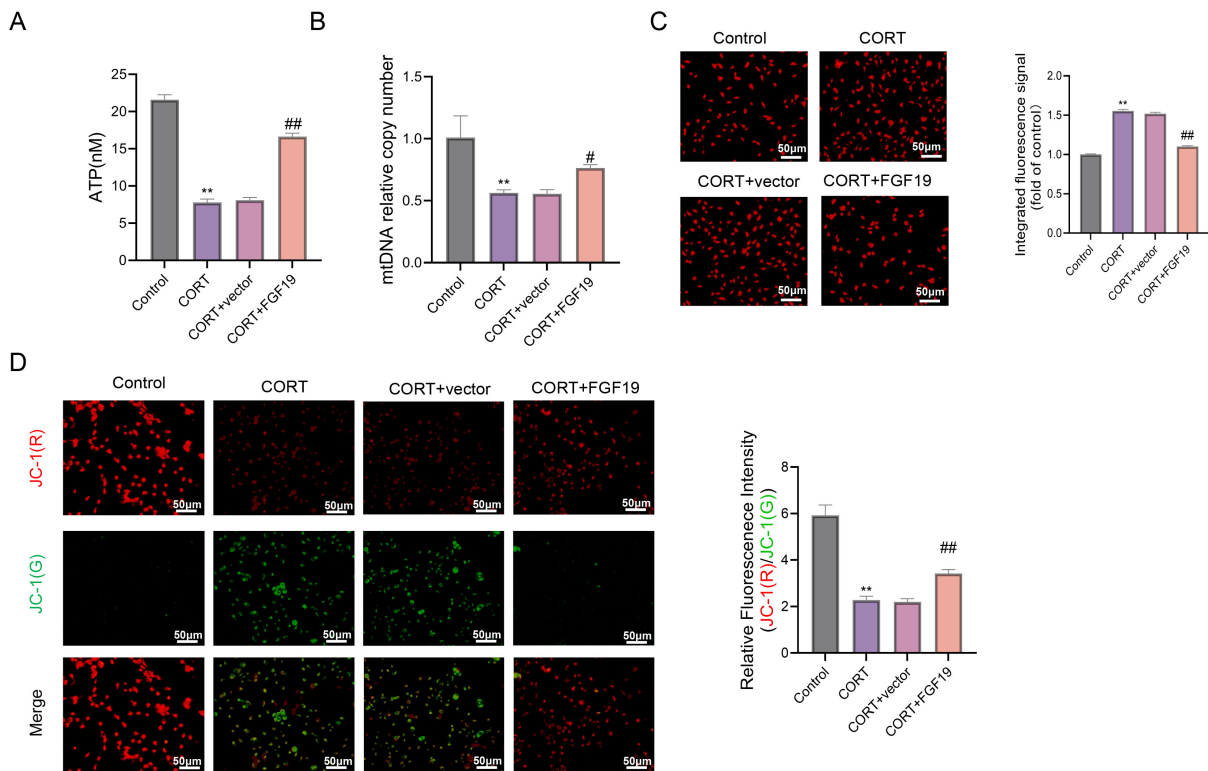


**Fig. 4. FGF19 overexpression ameliorates cortisol-induced mitochondrial dysfunction in AC16 cells.** (A) Intracellular adenosine triphosphate (ATP) levels. (B) Relative mitochondrial DNA (mtDNA) copy number. (C) Mitochondrial reactive oxygen species (ROS) levels quantified by fluorescence intensity. (D) Representative JC-1 staining images assessing mitochondrial membrane potential; red fluorescence (JC-1 aggregates) indicates polarized mitochondria, green fluorescence (JC-1 monomers) indicates depolarized mitochondria. Scale bar = 50  $\mu$ m. Data are presented as mean  $\pm$  SD (n = 3). \*\* $p$  < 0.01 vs. Control; # $p$  < 0.05, ## $p$  < 0.01 vs. CORT + vector.

Collectively, these results confirm that FGF19 expression is downregulated by cortisol in a time-dependent manner and can be reliably manipulated at both the mRNA and protein levels, establishing a robust model for subsequent functional analyses.

#### *FGF19 Modulates Cortisol-Induced Injury and Apoptosis in AC16 Cells*

To evaluate the functional role of FGF19 in cortisol-induced cardiomyocyte injury, both overexpression and knockdown approaches were employed in AC16 cells.

FGF19 overexpression significantly alleviated cellular damage triggered by cortisol. As shown in Fig. 2A,B, treatment with cortisol increased the release of LDH and CK-MB, markers of membrane integrity loss and myocardial injury ( $p$  < 0.01). These elevations were significantly suppressed in the CORT + FGF19 group compared to the CORT + vector group ( $p$  < 0.01). Additionally, MTT assay revealed that cortisol significantly impaired cell viability, which was restored by FGF19 overexpression ( $p$  < 0.01; Fig. 2C). TUNEL staining further showed a significant reduction in the apoptotic rate in the FGF19-overexpressing group ( $p$  < 0.01; Fig. 2D). Western blot analysis confirmed

that FGF19 decreased the expression of pro-apoptotic proteins Bax and cleaved caspase-3, while upregulating anti-apoptotic Bcl-2 levels ( $p$  < 0.01; Fig. 2E).

Conversely, FGF19 knockdown exacerbated cortisol-induced cellular injury. As shown in Fig. 3A,B, siRNA-mediated silencing of FGF19 significantly increased LDH and CK-MB levels compared to the CORT + si-NC group ( $p$  < 0.01), indicating aggravated cell membrane damage. Consistently, the MTT assay revealed a further reduction in cell viability in the CORT + si-FGF19 group (Fig. 3C). TUNEL staining demonstrated a marked increase in apoptosis in FGF19-deficient cells under cortisol treatment ( $p$  < 0.01; Fig. 3D). Western blot analysis further confirmed the pro-apoptotic shift, with increased expression of Bax and cleaved caspase-3, and decreased Bcl-2 levels in the CORT + si-FGF19 group ( $p$  < 0.05 or  $p$  < 0.01; Fig. 3E), indicating enhanced mitochondrial-mediated apoptosis.

Collectively, these findings suggest that FGF19 confers a protective effect against cortisol-induced cytotoxicity by maintaining membrane integrity and inhibiting apoptosis, whereas its depletion increases cellular susceptibility to stress-induced injury.

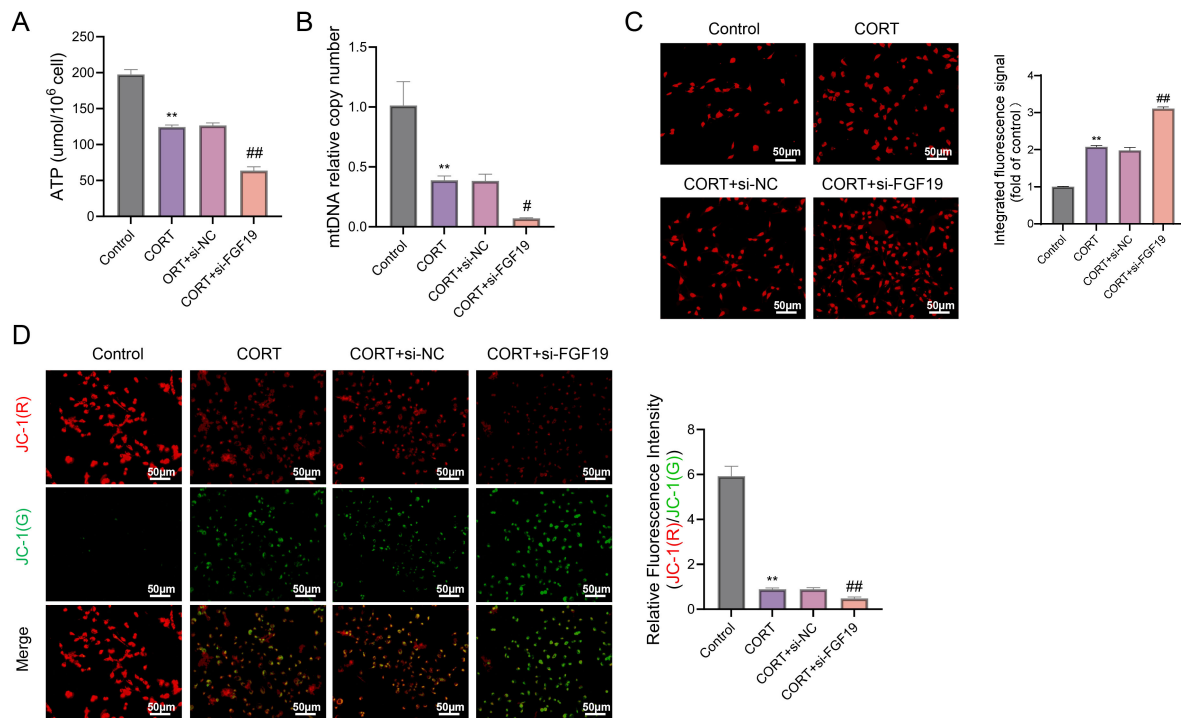


**Fig. 5. FGF19 knockdown aggravates cortisol-induced mitochondrial dysfunction in AC16 cells.** (A) Intracellular ATP levels. (B) Relative mitochondrial DNA (mtDNA) copy number. (C) Mitochondrial reactive oxygen species (ROS) levels quantified by fluorescence intensity. (D) Representative JC-1 staining images assessing mitochondrial membrane potential; red fluorescence (JC-1 aggregates) indicates polarized mitochondria, green fluorescence (JC-1 monomers) indicates depolarized mitochondria. Scale bar = 50  $\mu$ m. Data are presented as mean  $\pm$  SD ( $n = 3$ ). \*\* $p < 0.01$  vs. Control; # $p < 0.05$ , ## $p < 0.01$  vs. CORT + si-NC.

#### *FGF19 Preserves Mitochondrial Function Under Cortisol Stress in AC16 Cells*

To further elucidate the mitochondrial regulatory role of FGF19 under glucocorticoid stress, key indicators of mitochondrial function were assessed in AC16 cells. Cortisol exposure significantly impaired mitochondrial function, as demonstrated by decreased intracellular ATP levels, reduced mitochondrial DNA (mtDNA) copy number, and increased mitochondrial ROS production ( $p < 0.01$ ; Fig. 4A–C). Additionally, JC-1 staining revealed a marked loss of mitochondrial membrane potential in the CORT group, evidenced by a decreased red-to-green fluorescence ratio ( $p < 0.01$ ; Fig. 4D). Notably, FGF19 overexpression significantly reversed these effects, restoring ATP content, mtDNA copy number, and membrane potential, while suppressing ROS accumulation compared to the CORT + vector group ( $p < 0.05$  or  $p < 0.01$ ).

To confirm the endogenous protective role of FGF19, siRNA-mediated knockdown experiments were conducted. As shown in Fig. 5A,B, silencing of FGF19 exacerbated cortisol-induced mitochondrial dysfunction, causing further reductions in ATP production and mtDNA levels ( $p < 0.05$  or  $p < 0.01$ ). Moreover, mitochondrial ROS levels were significantly elevated, and JC-1 red/green fluorescence ratio was further decreased, indicating severe mitochondrial depolarization ( $p < 0.01$ ; Fig. 5C,D).

Collectively, these results demonstrate that FGF19 is critical for maintaining mitochondrial homeostasis and function in cardiomyocytes under cortisol-induced stress.

#### *FGF19 Modulates Mitochondrial Biogenesis and Fusion/Fission Dynamics in Cortisol-Treated AC16 Cells*

To investigate the regulatory role of FGF19 on mitochondrial homeostasis under cortisol-induced stress, the expression levels of key proteins involved in mitochondrial biogenesis and dynamics were evaluated. As shown in Fig. 6A, cortisol treatment significantly downregulated the expression of mitochondrial biogenesis markers PGC-1 $\alpha$  and TFAM, as well as mitochondrial fusion proteins Mfn1 and Mfn2 ( $p < 0.01$ ), while markedly upregulating the mitochondrial fission protein Drp1. Overexpression of FGF19 effectively reversed these changes, with the CORT + FGF19 group exhibiting significantly increased levels of PGC-1 $\alpha$ , TFAM, Mfn1, and Mfn2, along with reduced Drp1 expression compared to the CORT + vector group ( $p < 0.01$ ).

Conversely, siRNA-mediated knockdown of FGF19 exacerbated cortisol-induced dysregulation of these mitochondrial regulatory proteins. As shown in Fig. 6B, FGF19 silencing further decreased the expression of PGC-1 $\alpha$ , TFAM, Mfn1, and Mfn2, and increased Drp1 levels relative to the CORT + si-NC group ( $p < 0.05$  or  $p < 0.01$ ).

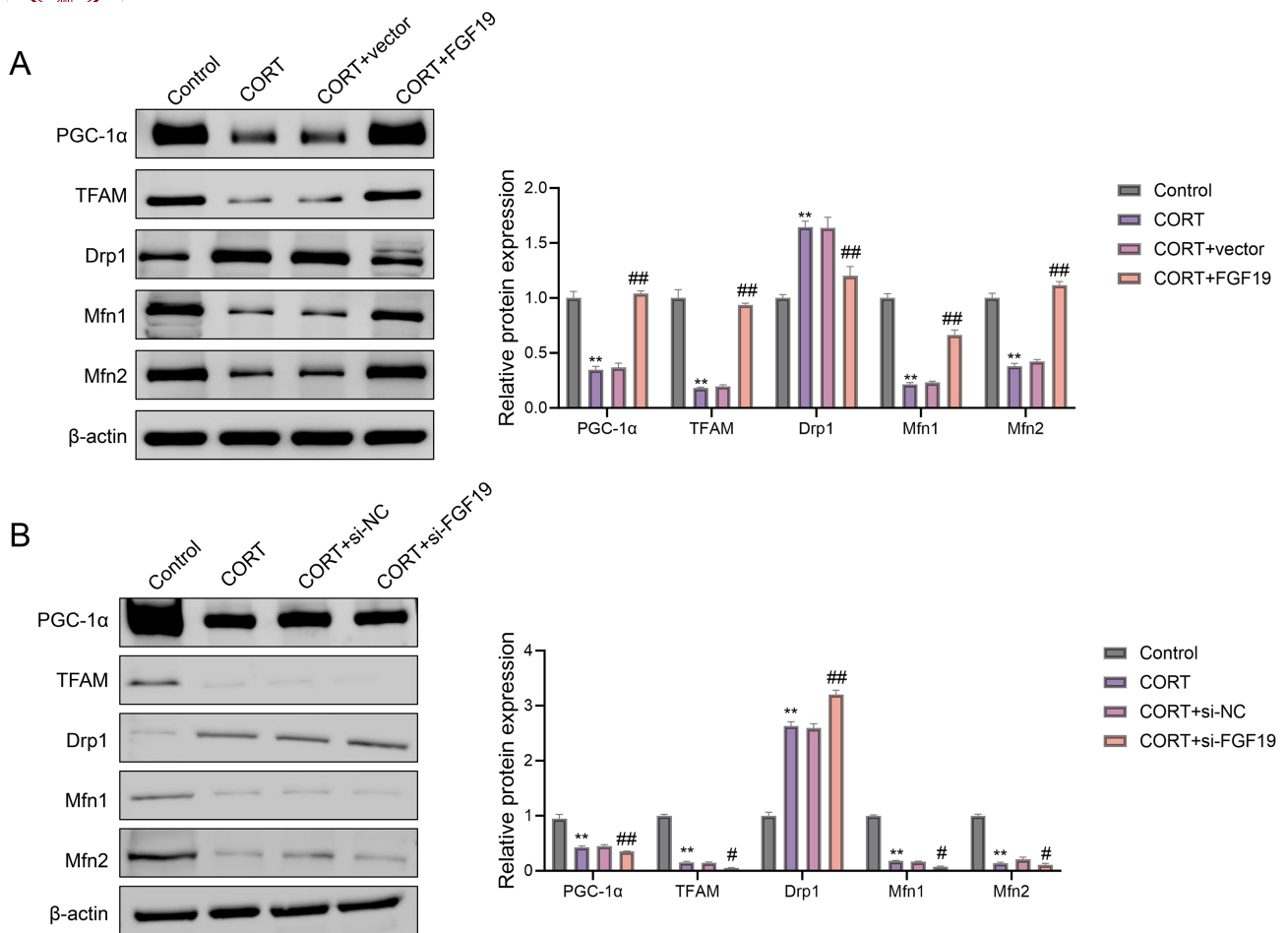


**Fig. 6. FGF19 regulates the expression of mitochondrial biogenesis and fusion/fission-related proteins in cortisol-treated AC16 cells.** (A) Western blot analysis of PGC-1 $\alpha$ , TFAM, Drp1, Mfn1, and Mfn2 protein levels in cortisol-treated cells transfected with FGF19 overexpression or vector. (B) Western blot analysis of the same mitochondrial regulatory proteins in cortisol-treated cells transfected with si-FGF19 or si-NC. Data are presented as mean  $\pm$  SD (n = 3). \*\* $p$  < 0.01 vs. Control; # $p$  < 0.05, ## $p$  < 0.01 vs. CORT + vector or CORT + si-NC. PGC-1 $\alpha$ , peroxisome proliferator-activated receptor gamma coactivator 1-alpha; TFAM, mitochondrial transcription factor A; Drp1, dynamin-related protein 1; Mfn, mitofusins.

These results demonstrate that FGF19 is crucial for maintaining mitochondrial integrity under glucocorticoid stress by promoting mitochondrial biogenesis and fusion, while suppressing excessive mitochondrial fission.

### Discussion

This study demonstrates for the first time that FGF19 protects human AC16 cardiomyocytes from cortisol-induced mitochondrial dysfunction and apoptosis. Cortisol-mediated downregulation of FGF19 was associated with impaired mitochondrial biogenesis, disrupted fusion–fission dynamics, increased oxidative stress, and activation of pro-apoptotic pathways. These findings reveal a previously unrecognized role for FGF19 as a critical regulator of mitochondrial integrity and cellular survival under glucocorticoid stress.

As a key effector of the hypothalamic–pituitary–adrenal axis, cortisol has been widely implicated in stress-

related cardiovascular pathology through its capacity to disrupt mitochondrial function, elevate ROS production, and promote apoptotic cell death [23–25]. Our results suggest that FGF19 acts as an intrinsic modulator that counteracts cortisol-induced mitochondrial dysfunction, underscoring its potential therapeutic value in cardiac stress responses.

Mechanistically, FGF19 upregulation was associated with activation of mitochondrial biogenesis regulators PGC-1 $\alpha$  and TFAM, alongside restoration of fusion–fission dynamics through increased expression of Mfn1/2 and reduced Drp1 levels [26]. Maintaining this balance is essential for preserving mitochondrial integrity and preventing fragmentation, a process closely linked to cardiomyocyte apoptosis and contractile dysfunction [27,28]. These findings are consistent with previous reports on FGF21, a close homolog of FGF19, which activates antioxidant pathways and suppresses apoptosis in cardiomyocytes [13,14]. Building on this, our study shows that depletion of FGF19 exacer-

bates cortisol-induced injury, indicating a vital role for endogenous FGF19 in preserving mitochondrial quality control during glucocorticoid stress.

While the precise downstream signaling pathways remain to be fully elucidated, FGF19 is known to act through FGFR4/ $\beta$ -Klotho receptor complexes and may engage AMPK and SIRT1, key regulators of mitochondrial metabolism and oxidative stress responses [19]. However, since direct evidence was not obtained in this study, these mechanistic connections remain speculative and warrant further investigation employing pathway-specific inhibitors, activators, or genetic modulation approaches.

Beyond its role in mitochondrial regulation, FGF19 may also exert direct anti-apoptotic effects in cardiomyocytes. The observed modulation of apoptosis-related proteins—namely Bax, Bcl-2, and cleaved caspase-3—indicates that FGF19 helps maintain the balance between cell survival and death pathways under glucocorticoid stress. This aligns with prior studies reporting anti-apoptotic effects of FGF family members across various cellular contexts [29,30]. Furthermore, the reduction in LDH and CK-MB release supports the cytoprotective role of FGF19, as these biomarkers are well-established indicators of cellular injury and myocardial damage [31,32].

A notable strength of this study is the bidirectional gene manipulation approach. Previous research on FGF19 and its homologs largely relied on overexpression models [14,33], which, while valuable, did not fully address the impact of FGF19 loss. Our use of both gain- and loss-of-function strategies provides complementary evidence for the critical role of FGF19 in cardiomyocyte stress adaptation. Nevertheless, future studies involving additional stressors and *in vivo* validation will be essential to establish the broader applicability and translational relevance of these findings.

While this study provides novel insights into the protective role of FGF19 in cortisol-induced cardiomyocyte injury, several limitations should be noted. First, all experiments were conducted using AC16 cardiomyocytes, an immortalized human cell line that may not fully replicate the physiological properties of primary cardiomyocytes, highlighting the need for validation in primary cells and animal models. Second, the cortisol concentration applied was based on prior studies to induce mitochondrial stress; future dose-response analyses using clinically relevant concentrations are warranted. Third, although FGF19 overexpression and knockdown efficiencies were confirmed, the overexpression system may have produced supraphysiological FGF19 levels, potentially leading to non-specific effects. Fourth, the effects of FGF19 manipulation under basal (non-stressed) conditions were not examined, which would help clarify its role in maintaining homeostasis.

Additionally, this study utilized a single *in vitro* model and did not assess whether FGF19 exerts similar protective effects under other stressors such as norepinephrine, oxidative agents, or alternative glucocorticoids. Functional end-

points including contractility, calcium handling, and cardiac biomarkers (e.g., cTnI, BNP) were also not evaluated. Finally, although the AMPK/SIRT1 pathway was proposed as a potential mediator, direct evidence was lacking, and the duration and reversibility of FGF19's protective effects remain unknown. Future studies employing functional assays, pathway-specific interventions, and *in vivo* models will be essential to determine the therapeutic potential of FGF19 in stress-related cardiac disorders.

## Conclusion

This study demonstrates that FGF19 protects cardiomyocytes from cortisol-induced mitochondrial dysfunction and apoptosis by enhancing mitochondrial biogenesis, restoring mitochondrial dynamics, and mitigating oxidative stress. These findings highlight FGF19 as a promising therapeutic target for stress-related cardiac injury, although further investigations are necessary to validate its clinical potential.

## Availability of Data and Materials

The data used to support the findings of this study are available from the corresponding author upon request.

## Author Contributions

JZ: Conceptualization; Data curation; Formal analysis; Investigation; Visualization; Writing - original draft; Writing - review & editing. XM: Conceptualization; Data curation; Formal analysis; Investigation; Methodology; Resources; Writing - original draft; Writing - review & editing. Both authors contributed to important editorial changes in the manuscript. Both authors read and approved the final manuscript. Both authors have participated sufficiently in the work and agreed to be accountable for all aspects of the work.

## Ethics Approval and Consent to Participate

Not applicable.

## Acknowledgment

Not applicable.

## Funding

This research received no external funding.

## Conflict of Interest

The authors declare no conflict of interest.

## Supplementary Material

Supplementary material associated with this article can be found, in the online version, at <https://doi.org/10.24976/Descov.Med.202537201.189>.

### References

- [1] Park HY, Lee HW, Song GJ, Hong S, Hong S, Suh HW, *et al.* Systematic review and meta-analysis of cardiac neurosis for development of clinical practice guidelines of Korean medicine. *Frontiers in Psychiatry*. 2024; 15: 1302245. <https://doi.org/10.3389/fpsy.2024.1302245>.
- [2] Zheng F, Duan Y, Li J, Lai L, Zhong Z, Hu M, *et al.* Somatic symptoms and their association with anxiety and depression in Chinese patients with cardiac neurosis. *The Journal of International Medical Research*. 2019; 47: 4920–4928. <https://doi.org/10.1177/0300060519869711>.
- [3] McEwen BS. Physiology and neurobiology of stress and adaptation: central role of the brain. *Physiological Reviews*. 2007; 87: 873–904. <https://doi.org/10.1152/physrev.00041.2006>.
- [4] Dedovic K, Duchesne A, Andrews J, Engert V, Pruessner JC. The brain and the stress axis: the neural correlates of cortisol regulation in response to stress. *NeuroImage*. 2009; 47: 864–871. <https://doi.org/10.1016/j.neuroimage.2009.05.074>.
- [5] Brdiczka DG, Zorov DB, Sheu SS. Mitochondrial contact sites: their role in energy metabolism and apoptosis. *Biochimica et Biophysica Acta*. 2006; 1762: 148–163. <https://doi.org/10.1016/j.bbdis.2005.09.007>.
- [6] Yang S, Lian G. ROS and diseases: role in metabolism and energy supply. *Molecular and Cellular Biochemistry*. 2020; 467: 1–12. <https://doi.org/10.1007/s11010-019-03667-9>.
- [7] Vakifahmetoglu-Norberg H, Ouchida AT, Norberg E. The role of mitochondria in metabolism and cell death. *Biochemical and Biophysical Research Communications*. 2017; 482: 426–431. <https://doi.org/10.1016/j.bbrc.2016.11.088>.
- [8] Zhou B, Tian R. Mitochondrial dysfunction in pathophysiology of heart failure. *The Journal of Clinical Investigation*. 2018; 128: 3716–3726. <https://doi.org/10.1172/JCI120849>.
- [9] Xu Y, Wang P, Hu T, Ning K, Bao Y. Notoginsenoside R1 Attenuates H/R Injury in H9c2 Cells by Maintaining Mitochondrial Homeostasis. *Current Issues in Molecular Biology*. 2025; 47: 44. <https://doi.org/10.3390/cimb47010044>.
- [10] Vásquez-Trincado C, García-Carvajal I, Pennanen C, Parra V, Hill JA, Rothermel BA, *et al.* Mitochondrial dynamics, mitophagy and cardiovascular disease. *The Journal of Physiology*. 2016; 594: 509–525. <https://doi.org/10.1113/JP271301>.
- [11] Song M, Mihara K, Chen Y, Scorrano L, Dorn GW, 2nd. Mitochondrial fission and fusion factors reciprocally orchestrate mitophagic culling in mouse hearts and cultured fibroblasts. *Cell Metabolism*. 2015; 21: 273–286. <https://doi.org/10.1016/j.cmet.2014.12.011>.
- [12] Dolegowska K, Marchelek-Mysliwiec M, Nowosiad-Magda M, Slawinski M, Dolegowska B. FGF19 subfamily members: FGF19 and FGF21. *Journal of Physiology and Biochemistry*. 2019; 75: 229–240. <https://doi.org/10.1007/s13105-019-00675-7>.
- [13] Planavila A, Redondo-Angulo I, Ribas F, Garrabou G, Casademont J, Giral M, *et al.* Fibroblast growth factor 21 protects the heart from oxidative stress. *Cardiovascular Research*. 2015; 106: 19–31. <https://doi.org/10.1093/cvr/cvu263>.
- [14] Fang Y, Zhao Y, He S, Guo T, Song Q, Guo N, *et al.* Overexpression of FGF19 alleviates hypoxia/reoxygenation-induced injury of cardiomyocytes by regulating GSK-3 $\beta$ /Nrf2/ARE signaling. *Biochemical and Biophysical Research Communications*. 2018; 503: 2355–2362. <https://doi.org/10.1016/j.bbrc.2018.06.161>.
- [15] Itoh N, Ornitz DM. Fibroblast growth factors: from molecular evolution to roles in development, metabolism and disease. *Journal of Biochemistry*. 2011; 149: 121–130. <https://doi.org/10.1093/jb/mvq121>.
- [16] Chen K, Rao Z, Dong S, Chen Y, Wang X, Luo Y, *et al.* Roles of the fibroblast growth factor signal transduction system in tissue injury repair. *Burns & Trauma*. 2022; 10: tkac005. <https://doi.org/10.1093/burnst/tkac005>.
- [17] Farooq M, Khan AW, Kim MS, Choi S. The Role of Fibroblast Growth Factor (FGF) Signaling in Tissue Repair and Regeneration. *Cells*. 2021; 10: 3242. <https://doi.org/10.3390/cell10113242>.
- [18] Cheng CF, Ku HC, Lin H. PGC-1 $\alpha$  as a Pivotal Factor in Lipid and Metabolic Regulation. *International Journal of Molecular Sciences*. 2018; 19: 3447. <https://doi.org/10.3390/ijms19113447>.
- [19] Guo A, Li K, Tian HC, Fan Z, Chen QN, Yang YF, *et al.* FGF19 protects skeletal muscle against obesity-induced muscle atrophy, metabolic derangement and abnormal irisin levels via the AMPK/SIRT-1/PGC- $\alpha$  pathway. *Journal of Cellular and Molecular Medicine*. 2021; 25: 3585–3600. <https://doi.org/10.1111/jcmm.16448>.
- [20] Faul C. Cardiac actions of fibroblast growth factor 23. *Bone*. 2017; 100: 69–79. <https://doi.org/10.1016/j.bone.2016.10.001>.
- [21] Thakur V, Alcoreza N, Cazares J, Chattopadhyay M. Changes in Stress-Mediated Markers in a Human Cardiomyocyte Cell Line under Hyperglycemia. *International Journal of Molecular Sciences*. 2021; 22: 10802. <https://doi.org/10.3390/ijms221910802>.
- [22] ZhiQing Z, XinXing W, Jingbo G, Rui Z, Xiujie G, Yun Z, *et al.* Effects of HIP in protection of HSP70 for stress-induced cardiomyocytes injury and its glucorticoid receptor pathway. *Cell Stress & Chaperones*. 2014; 19: 865–875. <https://doi.org/10.1007/s12192-014-0510-y>.
- [23] Chen QM, Alexander D, Sun H, Xie L, Lin Y, Terrand J, *et al.* Corticosteroids inhibit cell death induced by doxorubicin in cardiomyocytes: induction of antiapoptosis, antioxidant, and detoxification genes. *Molecular Pharmacology*. 2005; 67: 1861–1873. <https://doi.org/10.1124/mol.104.003814>.
- [24] Pearl JM, Nelson DP, Schwartz SM, Wagner CJ, Bauer SM, Setser EA, *et al.* Glucocorticoids reduce ischemia-reperfusion-induced myocardial apoptosis in immature hearts. *The Annals of Thoracic Surgery*. 2002; 74: 830–836; discussion 836–837. [https://doi.org/10.1016/s0003-4975\(02\)03843-2](https://doi.org/10.1016/s0003-4975(02)03843-2).
- [25] Rog-Zielinska EA, Craig MA, Manning JR, Richardson RV, Gowans GJ, Dunbar DR, *et al.* Glucocorticoids promote structural and functional maturation of foetal cardiomyocytes: a role for PGC-1 $\alpha$ . *Cell Death and Differentiation*. 2015; 22: 1106–1116. <https://doi.org/10.1038/cdd.2014.181>.
- [26] Fontecha-Barruso M, Martin-Sanchez D, Martinez-Moreno JM, Monsalve M, Ramos AM, Sanchez-Niño MD, *et al.* The Role of PGC-1 $\alpha$  and Mitochondrial Biogenesis in Kidney Diseases. *Biomolecules*. 2020; 10: 347. <https://doi.org/10.3390/biom10020347>.
- [27] Chen S, Li Q, Shi H, Li F, Duan Y, Guo Q. New insights into the role of mitochondrial dynamics in oxidative stress-induced diseases. *Biomedicine & Pharmacotherapy*. 2024; 178: 117084. <https://doi.org/10.1016/j.biopha.2024.117084>.
- [28] Hu L, Ding M, Tang D, Gao E, Li C, Wang K, *et al.* Targeting mitochondrial dynamics by regulating Mfn2 for therapeutic intervention in diabetic cardiomyopathy. *Theranostics*. 2019; 9: 3687–3706. <https://doi.org/10.7150/thno.33684>.
- [29] Ren C, Chen H, Han C, Fu D, Wang F, Wang D, *et al.* The anti-apoptotic and prognostic value of fibroblast growth factor 9 in gastric cancer. *Oncotarget*. 2016; 7: 36655–36665. <https://doi.org/10.18632/oncotarget.9131>.
- [30] Kostas M, Lampart A, Bober J, Wiedlocha A, Tomala J, Krowarsch D, *et al.* Translocation of Exogenous FGF1 and

FGF2 Protects the Cell against Apoptosis Independently of Receptor Activation. *Journal of Molecular Biology*. 2018; 430: 4087–4101. <https://doi.org/10.1016/j.jmb.2018.08.004>.

- [31] Apple FS, Voss E, Lund L, Preese L, Berger CR, Henry TD. Cardiac troponin, CK-MB and myoglobin for the early detection of acute myocardial infarction and monitoring of reperfusion following thrombolytic therapy. *Clinica Chimica Acta; International Journal of Clinical Chemistry*. 1995; 237: 59–66. [https://doi.org/10.1016/0009-8981\(95\)06064-k](https://doi.org/10.1016/0009-8981(95)06064-k).
- [32] Chen M, Wang M, Yang Q, Wang M, Wang Z, Zhu Y, *et al.*

Antioxidant effects of hydroxysafflor yellow A and acetyl-11-keto- $\beta$ -boswellic acid in combination on isoproterenol-induced myocardial injury in rats. *International Journal of Molecular Medicine*. 2016; 37: 1501–1510. <https://doi.org/10.3892/ijmm.2016.2571>.

- [33] Zhu Z, Hu B, Zhu D, Li X, Chen D, Wu N, *et al.* Bromocriptine sensitivity in bromocriptine-induced drug-resistant prolactinomas is restored by inhibiting FGF19/FGFR4/PRL. *Journal of Endocrinological Investigation*. 2025; 48: 67–80. <https://doi.org/10.1007/s40618-024-02408-0>.